Development of a 6-axis robot's finger force/moment sensor for stable grasping of an unknown object

Gab-Soon Kim[1,#]

[1] RICIC, Department of Control & Instrumentation Engineering, Gyeongsang National University, Jinju, South Korea

ABSTRACT

This paper describes the development of a 6-axis robot's finger force/moment sensor, which measures forces F_x (x-direction force), F_y and F_z, and moments M_x (x-direction moment), M_y and M_z simultaneously, for stable grasping of an unknown object. In order to safely grasp an unknown object using the robot's gripper, the force in the gripping direction and the force in the gravity direction should be measured, and the force control should be performed using the measured forces. Also, the moments M_x, M_y and M_z to accurately perceive the position of the object in the grippers should be detected. Thus, the robot's gripper should be composed of 6-axis robot's finger force/moment sensor that can measure forces F_x, F_y and F_z, and moments M_x, M_y and M_z simultaneously. In this paper, the 6-axis robot's finger force/moment sensor for measuring forces F_x, F_y and F_z, and moments M_x, M_y and M_z simultaneously was newly modeled using several parallel-plate beams, designed, and fabricated. The characteristic test of the fabricated sensor was performed, and the result shows that interference errors of the developed sensor are less than 3%. Also, Robot's gripper with the 6-axis robot's finger force/moment sensor for the characteristic test of force control was manufactured, and the characteristic test for grasping an unknown object using the sensors was performed using it. The fabricated gripper could grasp an unknown object stably. Thus, the developed 6-axis robot's finger force/moment sensor can be used for robot's gripper.

Key Words : Robot's gripper, 6-axis robot's finger force/moment sensor, Parallel-plate beam, Rated strain, Interference error

1. Introduction

Grippers for intelligent robots have been widely studied recently. Ceccarelli[1] made a robot's finger with a force sensor that can only detect the force in the grasping direction, and equipped it with position and force controls for gripping an unknown object. Castro[2] manufactured a jaw gripper with a F_x force sensor and carried out force control using it. Tlale[3] fabricated an intelligent gripper with a contact sensor and a circuit for controlling it. Carlos[4] fabricated a 3-finger gripper with a vision system. And, Obrien[5] manufactured a gripper that can only measure the force in the grasping direction.

The above grippers can't stably grasp an unknown object and also accurately perceive the position of the object in the grippers, because they can't detect the forces F_x, F_y and F_z, and the moments M_x, M_y and M_z, simultaneously. To safely grasp an unknown object, an intelligent robot's gripper needs to detect the forces in the gripping direction and in the gravitational direction, and it also needs to detect the moments to accurately perceive the position of the object in the grippers. Thus, the robot's gripper should be composed of a 6-axis force/moment sensor which can detect the forces F_x, F_y and F_z, and moments M_x, M_y and M_z, simultaneously.

To accurately measure forces and moments, a 6-axis force/moment sensor should have an interference error

☞ Manuscript received: January 6, 2004 ;
Accepted: March 18, 2004

Corresponding Author:
Email: gskim@gsnu.ac.kr
Tel: +82-55-751-5372, Fax: +82-55-757-3974

about 3 % ~ 15 %. The precision accuracy of the 6-axis force/moment sensor can be estimated by nonlinarity, repeatability and interference error. However, as the interference error is tens or hundreds times larger than the other errors, the precision accuracy is usually estimated by the interference error.[6-9]

In this paper, a 6-axis force/moment sensor of an intelligent robot's gripper for safe grasping of an unknown object and accurate perception of the position of the object in the grippers is developed. The structure of the 6-axis force/moment sensor having each sensor with the same or the different capacity is newly modeled using PPBs (parallel-plate beams). The equations for designing the sensing element of each sensor are derived. As a sample, the 6-axis force/moment sensor which can detect the forces F_x, F_y and F_z (maximum capacity of each is 50 N) and moments M_x, M_y and M_z (maximum capacity of each is 5 Nm) simultaneously is designed using the derived equations, and fabricated with strain gages. Finally, a characteristic test of the manufactured 6-axis force/moment sensor is performed, and the response characteristic test of PI (proportional and integral) force control for the intelligent robot's gripper system is evaluated.

2. Design of sensor

2.1 Modeling of the sensor

Fig. 1 shows the structure of newly modeled the 6-axis force/moment sensor which can detect the forces F_x, F_y and F_z, and the moments M_x, M_y and M_z for the intelligent robot's gripper system. The sensing elements of the 6-axis force/moment sensor are made by fixing E block part of two sensors with screws. One is a 5-axis force/moment sensor, which is compose of the F_x, F_y and F_z sensors and the M_x and M_y sensor, the other is the M_z sensor. Blocks A and B, and C and D are fixed to the frame of gripper with screws used to make the gripper.

The sensing elements of the F_x sensor and the M_y sensor are PPB (parallel-plate beams) 1 and 2, those of the F_y sensor and the M_x sensor are PPB 3 and 4, that of the F_z sensor is PPB 5, and those of the M_z sensor are PPB 6 and 7. PPB 1, 2, 3 and 4 are composed of two plate beams with width b_1, heights t_1 and t_1', length l_1, and the distance of the central line to the end of the beams d_1, d_2, d_3 and d_4, respectively. PPB 5 has width b_2, height t_2, length l_2, and distance d_5, d_6, and PPB 6 and 7 have b_3, t_3, l_3, d_7 and d_8, respectively.

As shown in Fig. 1, the PPB 1~7 are symmetric about the x-axis, y-axis and z-axis. The forces and the moments are applied to the plate beams through the lower load-transmitting block A and B that are located in the lower part, and the upper load-transmitting blocks C and D that are located in the upper part of the 6-axis force/moment sensor.

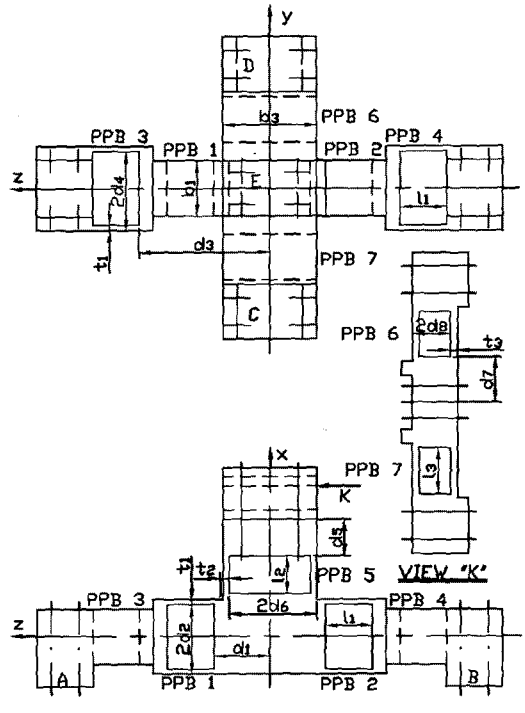

Fig. 1 6-axis robot's finger force/moment sensor

2.2 Theoretical analysis

2.2.1 Under the applied force F_x or F_y

Fig. 2 shows the free body diagram of the plate beams for the F_x sensor or the F_y sensor under the force F_x or F_y. PPB 1 and 2 are symmetric about the vertical axis (x-axis) and the horizontal axis (z-axis); the plate beam 3 and beam 4 are symmetric about the horizontal axis. Thus, the equations for analyzing the strains are derived on the upper and the lower surfaces of the plate beam 1, and these may be applied to the plate beam 2, 3 and 4. The equations under the force F_x may be applied to PPB 3 and 4 for the F_y sensor, because

PPB 1, 2 and 3, 4 have the same structure.

When the force F_x is applied to the block between PPB 1 and 2, the force F_{Fxx} applied to plate beam 1 along the x-direction at point $z=0$ is derived, and the moment M_{Fxy} applied to plate beam 1 along the y-direction at point O is derived using the moment equilibrium condition $\sum M_o = 0$. The moment M_{oz} at arbitrary point z can be derived using the force F_{Fxx} and the moment M_{Fxy}, and is[9,10]

$$M_{oz} = \frac{F_x}{4}(z - \frac{l_1}{2}) \tag{1}$$

The equations for analyzing the rated strains on the surfaces of the plate beam 1 are derived by substituting equation (1) into the bending equation $\varepsilon = M_{oz}/EZ_{1P}$, which can be written as follows.

$$\varepsilon_{Fx-U} = \frac{F_x}{4EZ_{1p}}(z - \frac{l_1}{2}) \tag{2-a}$$

$$\varepsilon_{Fx-L} = \frac{F_x}{4EZ_{1p}}(\frac{l_1}{2} - z) \tag{2-b}$$

where ε_{Fx-U} is the strain produced on the upper surface of each plate beam 1, and ε_{Fx-L} is the strain produced on the lower surface of each plate beam 1.

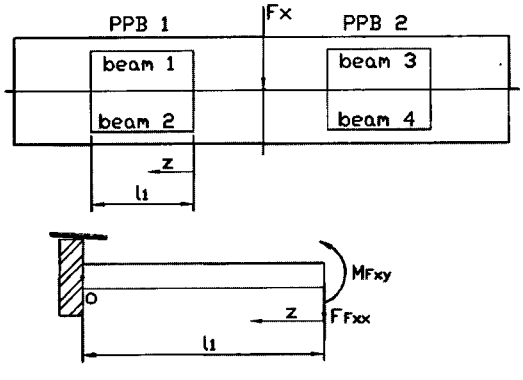

Fig. 2 Free body diagram of plate beams for a 6-axis robot's finger force/moment sensor under the forces F_x (or F_y)

2.2.2 Under the applied force F_z

Fig. 3 shows the free body diagram of the plate beams for the F_z sensor under the force F_z. PPB 5 comprises of the plate beams 5 and 6, and they are symmetric about the horizontal axis (y-axis) and are the same size. Thus, the equations for analyzing the strains are derived on the upper and the lower surfaces of the plate beam 5, and these may be applied to the plate beam 6.

When the force F_z is applied to the block end O_2, the force F_{Fzz} applied to plate beam 5 along the z-direction and the moment M_{Fzy} applied to plate beam 5 along the y-direction are derived, and the equations of the force equilibrium condition $\sum F_z = 0$ and the moment equilibrium condition $\sum M_o = 0$ are derived. The rotational angle ϕ and the vertical displacement v can be derived using the derived equations, and which leads to.[9,10]

$$\phi = \frac{(2d_4 + l_2)F_z}{\frac{48EI_2}{{l_2}^2}(\frac{3}{2}d_4 + \frac{2}{3}l_2) + \frac{4A_2Ed_5^2}{l_2}} \tag{3}$$

$$v = \frac{F_z - \frac{24EI_2}{{l_2}^2}(d_4 + \frac{l_2}{2})\phi}{\frac{24EI_2}{{l_2}^2}} \tag{4}$$

where I_2 is the moment inertia of the area of plate beam 2, and A_2 is the area of plate beam 2.

The moment M_{ox} at arbitrary point x on the plate beam 5 can be written

$$M_{ox} = F_{Fzz}x - M_{Fzy} = \frac{12EI_2x}{{l_2}^3}\left[v + (d_4 + \frac{l_2}{2})\phi\right] - \frac{12EI_2}{{l_2}^2}\left[\frac{v}{2} + (\frac{d_4}{2} + \frac{l_2}{3})\phi\right] \tag{5}$$

where v is the vertical displacement.

The equations for analyzing the rated strains on the surfaces of the plate beam 5 are derived using the bending equation $\varepsilon = M_{ox}/EZ_{2P}$, and the tension and compression strain equations $\varepsilon = F/A_2E$, which can be written as

$$\varepsilon_{Fz-U} = \frac{6t_2x}{{l_2}^3}(v + (d_4 + \frac{l_2}{2})\phi) - \frac{6t_2}{{l_2}^2}(\frac{v}{2} + (\frac{d_4}{2} + \frac{l_2}{3})\phi) + \frac{d_5\phi}{l_2} \tag{6-a}$$

$$\varepsilon_{Fz-L} = -\frac{6t_2 x}{l_2^3}(v+(d_4+\frac{l_2}{2})\phi) + \frac{6t_2}{l_2^2}(\frac{v}{2}+(\frac{d_4}{2}+\frac{l_2}{3})\phi) - \frac{d_5\phi}{l_2} \quad (6\text{-b})$$

where Z_{2p} is the polar moment of inertia of of plate beam 2, ε_{Fz-U} is the strains produced on the upper surface of each plate beam 5, and ε_{Fz-L} is the strains produced on the lower surface of each plate beam 5.

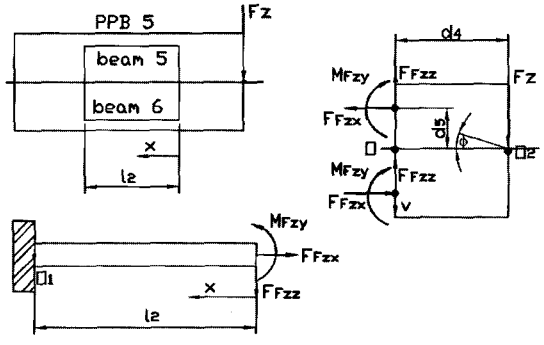

Fig. 3 Free body diagram of plate beams for a 6-axis robot's finger force/moment sensor under the force F_z

2.2.3 Under the applied moment M_x or M_y or M_z

Fig. 4 shows the free body diagram of the plate beams for the M_x sensor, the M_y sensor or the M_z sensor under the moment M_x or M_y or M_z. PPB 3 and 4 are symmetric about the vertical axis (y-axis), and the plate beams 7 and 8 are symmetric about the horizontal axis (z-axis), and also the plate beams 9 and 10 are symmetric about the horizontal axis (z-axis). Thus, the equations for analyzing the strains are derived on the upper and the lower surfaces of the plate beam 7, and these may be applied to the plate beams 8, 9 and 10. The equations under the moment M_x may be applied to PPB 1 and 2 for the M_y sensor and PPB 6 and 7 for the M_z sensor because these PPBs are same in the structure.

When the moment M_x is applied to the block center point P, the force F_{Mxz} applied to plate beam 7 along the z-direction, the force F_{Mxy} applied to the plate beam 7 along the y-direction, and the moment M_{Mxx} applied to the plate beam 7 along the x-direction are derived using the vertical displacement v and the rotational angle θ at the end point $z=0$ of the plate beam 7. Substituting these equations into the derived equation of the moment equilibrium condition $\sum M_P = 0$, the rotational angle θ at the center point P of the block between PPB 3 and 4 can be represented by the following equation.[9,10]

$$\theta = \frac{M_x/4}{\frac{12EI_1}{l_1^2}(d_1+\frac{l_1}{3}+\frac{d_1^2}{l_1})+\frac{A_1Ed_2^2}{l_1}} \quad (7)$$

The equations for analyzing the rated strains on the surfaces of the plate beam 7 are derived using the bending equation $\varepsilon = M/EZ_{1P}$, and the tension and compression strain equations $\varepsilon = F/A_1E$, which can be written as

$$\varepsilon_{Mx-U} = \left[\frac{6h}{l_1^3}\left(\frac{d_1l_1}{2}+\frac{l_1^2}{3}-(d_1+\frac{l_1}{2})x\right)+\frac{d_2}{l_1}\right]\theta \quad (8\text{-a})$$

$$\varepsilon_{Mx-L} = -\left[\frac{6h}{l_1^3}\left(\frac{d_1l_1}{2}+\frac{l_1^2}{3}-(d_1+\frac{l_1}{2})x\right)+\frac{d_2}{l_1}\right]\theta \quad (8\text{-b})$$

where ε_{Mx-U} is the strains produced on the upper surface of each plate beam 7, and ε_{Mx-L} is the strains produced on the lower surface of each plate beam 7.

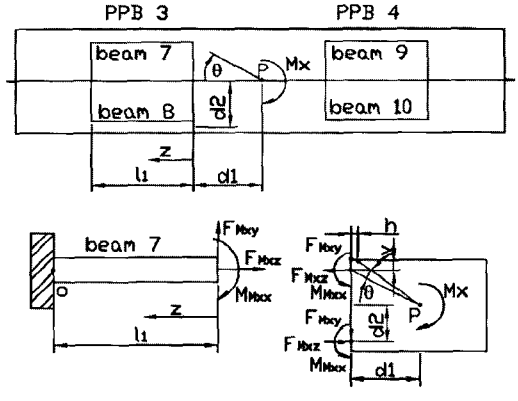

Fig. 4 Free body diagram of plate beams for a 6-axis robot's finger force/moment sensor under the moments M_x (or M_y, M_z)

2.3 Design of the sensing elements of each sensor

The sensing elements (PPBs) of each sensor in the 6-axis force/moment sensor are designed to have low

interference error. The design variables of each sensor are the rated capacity, the rated strain, the width, the length, the height of the plate beams, the distances from the central line to the end of the beam, and the location of strain gages considering the size of the strain gage.[6~10] The variables for designing the 6-axis force/moment sensor are determined as follows:

(1) The rated capacities of the F_x, F_y and F_z sensors are determined to be 50 N respectively, and those of the M_x, M_y and M_z sensors are 5 Nm respectively taking into consideration of the grasping force of the intelligent robot.

(2) The rated strains of each sensor are determined to be about 1000 $\mu m/m$ (about 0.5 mV/V) taking into consideration the same rated outputs and sensitivities in each sensor.

(3) The attachment locations of strain gages for all sensors are determined to be 1.5 mm from the end of the plate beams in the length direction, and the center of the plate beams in the width direction taking into consideration of the size of the strain gages used (1.52×2.54 mm^2).

The sizes of the sensing elements were calculated by substituting the determined variables into equations (2-a), (2-b), (6-a), (6-b), (8-a) and (8-b).

The sizes of the sensing elements in the rated capacities of $F_x = F_y = F_z$ =50 N, $M_x = M_y = M_z$ =5 Nm are as follows; the widths b_1, b_2 and b_3 are 12 mm, 12 mm and 20 mm, the lengths l_1, l_2 and l_3 are 10 mm, 8 mm and 10 mm, the heights (thickness) t_1, t_1', t_2 and t_3 are 1.1 mm, 1.1 mm, 1.3 mm and 1.2 mm, the distances d_1, d_2, d_3, d_4, d_5, d_6, d_7 and d_8 are 12 mm, 7.7 mm, 28mm, 8.6 mm, 10 mm, 10 mm, 10 mm and 4.8 mm respectively.

3. Strain analysis and Sensor manufacture

Fig. 5 shows the attachment locations of the strain gages for the 6-axis force/moment sensor. The attachment locations of strain gages for each sensor are as follows; the F_x sensor is S1, S2, S3 and S4, the F_y sensor is S5, S6, S7 and S8, the F_z sensor is S9, S10, S11, and S12, the M_x sensor is S13, S14, S15 and S16, the M_y sensor is S17, S18, S19 and S20, and the M_z sensor is S21, S22, S23 and S24.

The full bridge circuit for each sensor is constructed using the selected strain gages for each sensor as shown in Fig. 6. The rated strain and the interference strain are calculated using equation (9).

$$\varepsilon = \varepsilon_{T1} - \varepsilon_{C1} + \varepsilon_{T2} - \varepsilon_{C2} \tag{9}$$

where ε is the rated strain or the interference error, ε_{T1} is the strain from the tension strain gage T_1. ε_{T2} is the strain from the tension strain gage T_2. ε_{C1} is the strain from the compression strain gage C_1. ε_{C2} is the strain from the compression strain gage C_2.

Table 1 shows the rated strains and the interference errors of each sensor. The rated strain of the F_x, F_y and M_z sensors is 1032 $\mu m/m$ in the theoretical analysis, that of the F_z sensor is 1056 $\mu m/m$, for the M_x and M_y sensors are 1040 $\mu m/m$; the interference error of each sensor is 0 $\mu m/m$. Each sensor has a rated strain of more than 1000 $\mu m/m$, because the length and width of the sensing element are 1 mm units, and the thickness is 0.1 mm units. Each sensor has an interference error of 0 $\mu m/m$, because the attachment locations of strain gages are determined taking into consideration of the full bridge circuit, and the center of strain gage and the center of plate beam coincide. The strain gages (N2A-13-T001N-350) were attached to the selected attachment locations using a bond (M-bond 200) made by Micro-Measurement Company. The full bridge circuit for each sensor as shown in Fig. 6 was constructed using the strain gages.

Table 1 Rated strain and interference error of each sensor

	Rated strain and interference error ($\mu m/m$)					
Sensor / F/M	F_x	F_y	F_z	M_x	M_y	M_z
F_x=50 N	1032	0	0	0	0	0
F_y=50 N	0	1032	0	0	0	0
F_z=50 N	0	0	1056	0	0	0
M_x=5 Nm	0	0	0	1040	0	0
M_y=5 Nm	0	0	0	0	1040	0
M_z=5 Nm	0	0	0	0	0	1032

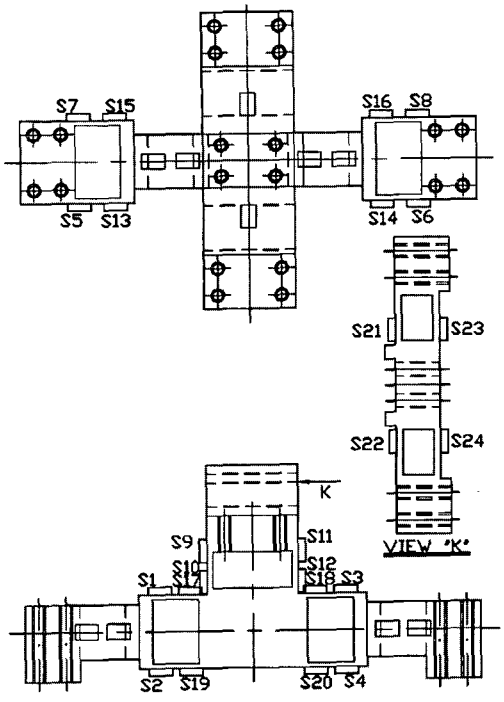

Fig. 5 Locations of strain gages

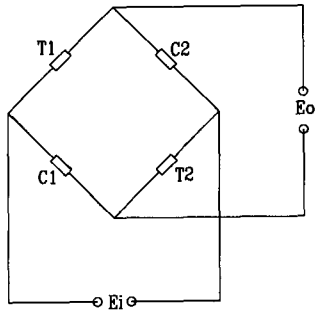

Fig. 6 Full bridge circuit

4. Result and consideration

Fig. 7 shows the experimental set up for the characteristic test of 6-axis force/moment sensor. It is composed of an arm, a weight, a body, a digital multi-meter (ADCANTEST, R6552), a power supply (UNICORN, UP-100DT). The manufactured 6-axis robot's finger force/moment sensor carried out the characteristic test using the experimental set up to evaluate its rated strains and interference errors. Each sensor was tested three times by using the experimental set up, and the output values from each sensor were averaged. In order to compare the rated strain in theory and the rated output in the characteristic test, the unit of the rated strain in theory ($\mu m / m$) should be changed into the unit of the rated output in characteristic test (mV / V); the equation for this is as follows,

$$\frac{E_o}{E_i} = \frac{1}{4} K\varepsilon \tag{10}$$

where E_i is the input voltage (V) of the full bridge circuit, E_o is the output voltage (V) of the full bridge circuit, K is the factor of strain gage (the used factor of strain gage is 2.03), and ε is the rated strain gage of each sensor ($\mu m / m$).

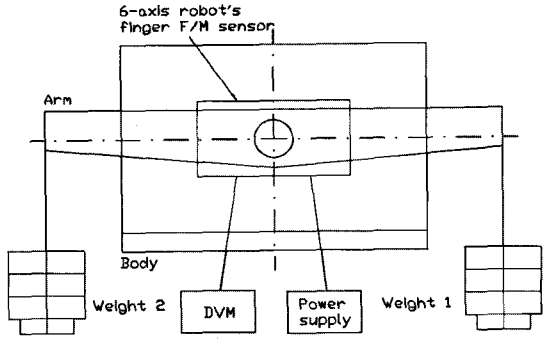

Fig. 7 Experimental set up for sensor for a characteristic test of 6-axis force/moment sensor

The rated strains ($\mu m / m$) in the theoretical analysis are changed into the rated output (mV / V) using the equation (10). Table 2 shows the rated outputs of each sensor from the theoretical analysis and the characteristic test. The maximum error of the rated strain from theoretical analysis compared with that from the characteristic test was less than 6.0 %. The error may be generated due to the processing error of the sensing element, the error of the characteristic test, the attachment error of the strain gage, and so on. Table 3 shows the interference errors from the characteristic test. The maximum interference error of the fabricated 6-axis force/moment sensor was below 2.79 %, and it is similar or less than that of the 6-axis force/moment sensor[1~10]. Fig. 8 shows a photograph of the developed 6-axis force/moment sensor.

Table 2 Rated strain in theory and characteristic test

Sensor	Analysis	Rated strain (mV/V)	Error(%)
F_x sensor	Theory	0.5237	6.0
	Test	0.4925	
F_y sensor	Theory	0.5237	4.5
	Test	0.5001	
F_z sensor	Theory	0.5396	4.0
	Test	0.5611	
M_x sensor	Theory	0.5278	3.3
	Test	0.5102	
M_y sensor	Theory	0.5278	3.4
	Test	0.5097	
M_z sensor	Theory	0.5237	4.6
	Test	0.4998	

Table 3 Interference errors in characteristic test

	Rated strain ($\mu m / m$) and Interference error (%)					
Sensor / F/M	F_x	F_y	F_z	M_x	M_y	M_z
F_x=50 N	-	-0.44	0.63	-0.05	-1.12	0.61
F_y=50 N	-0.77	-	-1.51	-2.12	-0.64	2.50
F_z=50 N	0.10	0.90	-	-0.46	1.84	0.74
M_x=5 Nm	-0.04	1.51	1.11	-	1.03	0.74
M_y=5 Nm	-0.70	-0.22	-0.48	1.76	-	1.73
M_z=5 Nm	-0.14	-2.45	2.20	-2.67	-2.79	-

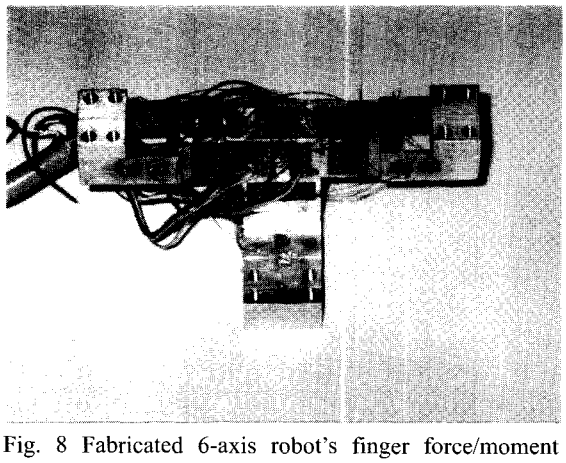

Fig. 8 Fabricated 6-axis robot's finger force/moment sensor

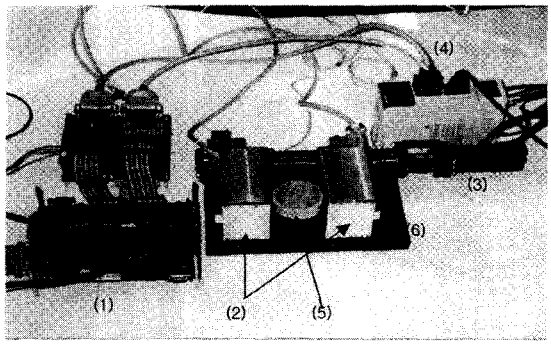

(1) Gripper controller, (2) Gripper(6-axis F/M sensor)
(3) Motor, (4) Motor driver, (5) Unknown object, (6) Body

Fig. 9 Robot's gripper with 6-axis robot's finger force/moment sensor

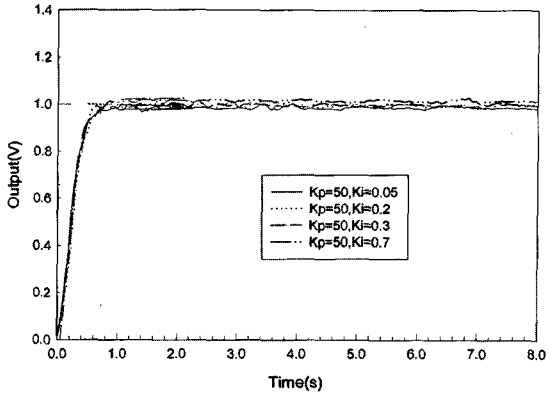

Fig. 10 Response of gripper with 6-axis robot's finger force/moment sensor

Fig. 9 shows the photograph of the developed gripper system. The gripper system comprises of a body, a gripper controller, a gripper 1 (6-axis force/moment sensor 1), a gripper 2 (6-axis force/moment sensor 2), a motor, a motor driver, a proximity sensor, a noise filter, and so on. The body consists of a screw, a fixture plate of gripper 1 and gripper 2, a flexible coupling, a base plate, and so on. The gripper 1 is fixed on the fixture plate of gripper 1, and the gripper 2 is fixed on the fixture plate of gripper 2.

The response characteristic test of PI force control of the developed gripper system was carried out to get the proportional gain K_p and the integral gain K_i. K_p with values ranging from 40 to 90 with 10 units was determined, K_i of 0.05, 0.1, 0.2, 0.3 and 0.5 was determined, and the sampling time was 0.05 s. As a result, the rising time is 0.4 s when K_p is 50. It is estimated

that PI force control is the best for grasping an object in the developed gripper system. Therefore, in this paper, the graph of the result is only shown.

Fig. 10 shows the response characteristic of PI force control of the developed gripper with 6-axis robot's finger force/moment sensor. The rising time is 0.4 s in K_i of 0.05, 0.1, 0.2, 0.3 and 0.5. The steady state deviations were calculated by the difference of the reference value and the output value. Each deviation was 0.012 V, 0.005 V, 0.003 V and –0.016 V when Ki are 0.05, 0.5, 0.3 and 0.5 respectively. The steady state errors, which were calculated by the fluctuation of the average outputs are ± 0.010 V, ± 0.006 V, ± 0.005 V and ± 0.005 V when Kis are 0.05, 0.2, 0.3 and 0.5 respectively. It is observed that the errors are developed from a control algorithm, a nose developed from motor and motor driver, and so on. As a result, it is estimated that the best response characteristic of the system is when K_p is 50 and K_i is 0.2.

5. Conclusion

This paper describes the development of a 6-axis robot's finger force/moment sensor, which detects forces F_x, F_y and F_z, and moments M_x, M_y and M_z simultaneously, for stable grasping of an unknown object.

As the results of the characteristic test of the fabricated 6-axis force/moment sensor, the maximum error of the rated strain and the maximum interference error were below 6.0 % and 2.79 % respectively. Thus, the derived equations (2-a), (2-b), (6-a), (6-b), (8-a) and (8-b) may be used for calculating the rated strains (designing the structure) of the modeled 6-axis force/moment sensor. It is observed that the fabricated 6-axis force/moment sensor can be used in an intelligent robot's gripper for stable grasping of an unknown object.

In the future, research on perceiving the position of the object in the grippers will be performed with a new testing system.

References

1. Ceccarelli, M., "Grasp Forces in Two-finger: Modeling and Measuring," Proceedings of 5th International Workshop on Robotics in Alpe Adria-Danbube Region, pp. 321-326, 1996.
2. Castro, D., "Tactile Force Control Feedback in Parallel Jaw Gripper," Proceedings of the IEEE International Symposium on Industrial Electronics, Vol. 3, No. 3, pp. 884-888, 1997.
3. Nkgatho, S. T., "intelligent Gripper using Low Cost Industrial," Proceedings of the IEEE International Symposium on Industrial Electronics, Vol. 2, No. 2, pp. 415-419, 1998.
4. Carlos, M. V., "BRF Competitive Hopfield Neural Networks for Objects Grasping," Proceedings of the Fourth International Conference on Motion and Vibration Control, Vol. 3, No. 3, pp. 1171-1176, 1998.
5. Obrien, D. J., "Force Explicit Slip Sensing for the Amadeus underwater Gripper," International Journal of Systems Science, Vol. 29, No. 5, pp. 471-483, 1998.
6. Yabuki, A., "Six-Axis Force/Torque Sensor for Assembly Robots," FUJTSU Science Technology, Vol. 26, No. 1, pp. 41-47, 1990.
7. Brussel, H. V., Belien, H., "Force Sensing for Advanced Robot Control," North-Holland Robotics2, pp. 139-148, 1986.
8. Lee, J., "Apply Force/Torque Sensors to Robotic Applications," North-Holland Robotics2, pp. 139-148, 1987.
9. Kim, G. S., "Design and fabrication of a three-component force/moment sensor using plate-beam," Meas. Sci. Technol., Vol. 10, pp. 295-301, 1999.
10. Kim, G. S., "Design of 3-component force/moment sensor with force/moment ratio of wide range," Korean Society Precision Engineering, Vol. 18, No. 2, pp. 214-221, 2001.